Clim Dyn
DOI 10.1007/s00382-009-0634-4

Impact of MJO on the intraseasonal variation of summer monsoon rainfall over India

D. S. Pai · Jyoti Bhate · O. P. Sreejith · H. R. Hatwar

Received: 12 April 2009 / Accepted: 10 July 2009

Abstract The summer monsoon rainfall over India exhibits strong intraseasonal variability. Earlier studies have identified Madden Julian Oscillation (MJO) as one of the most influencing factors of the intraseasonal variability of the monsoon rainfall. In this study, using India Meteorological Department (IMD) high resolution daily gridded rainfall data and Wheeler–Hendon MJO indices, the intra-seasonal variation of daily rainfall distribution over India associated with various Phases of eastward propagating MJO life cycle was examined to understand the mechanism linking the MJO to the intraseasonal variability. During MJO Phases of 1 and 2, formation of MJO associated positive convective anomaly over the equatorial Indian Ocean activated the oceanic tropical convergence zone (OTCZ) and the resultant changes in the monsoon circulation caused break monsoon type rainfall distribution. Associated with this, negative convective anomalies over monsoon trough zone region extended eastwards to date line indicating weaker than normal northern hemisphere inter tropical convergence zone (ITCZ). The positive convective anomalies over OTCZ and negative convective anomalies over ITCZ formed a dipole like pattern. Subsequently, as the MJO propagated eastwards to west equatorial Pacific through the maritime continent, a gradual northward shift of the OTCZ was observed and negative convective anomalies started appearing over equatorial Indian Ocean. During Phase 4, while the eastwards propagating MJO linked positive convective anomalies activated the eastern part of the ITCZ, the northward propagating OTCZ merged with monsoon trough (western part of the ITCZ) and induced positive convective anomalies over the region. During Phases 5 and 6, the dipole pattern in convective anomalies was reversed compared to that during Phases 1 and 2. This resulted active monsoon type rainfall distribution over India. During the subsequent Phases (7 and 8), the convective and lower tropospheric anomaly patterns were very similar to that during Phase 1 and 2 except for above normal convective anomalies over equatorial Indian Ocean. A general decrease in the rainfall was also observed over most parts of the country. The associated dry conditions extended up to northwest Pacific. Thus the impact of the MJO on the monsoon was not limited to the Indian region. The impact was rather felt over larger spatial scale extending up to Pacific. This study also revealed that the onset of break and active events over India and the duration of these events are strongly related to the Phase and strength of the MJO. The break events were relatively better associated with the strong MJO Phases than the active events. About 83% of the break events were found to be set in during the Phases 7, 8, 1 and 2 of MJO with maximum during Phase 1 (40%). On the other hand, about 70% of the active events were set in during the MJO Phases of 3 to 6 with maximum during Phase 4 (21%). The results of this study indicate an opportunity for using the real time information and skillful prediction of MJO Phases for the prediction of break and active conditions which are very crucial for agriculture decisions.

Keywords MJO · Monsoon · Rainfall · ITCZ

D. S. Pai (✉) · O. P. Sreejith · H. R. Hatwar
India Meteorological Department,
Shivaji Nagar, Pune 411005, India
e-mail: dspai@imdpune.gov.in

J. Bhate
National Atmospheric Research Laboratory,
Gadnki 517112, India

Published online: 06 August 2009

Abbreviations

MJO	Madden Julian Oscillation
OTCZ	Oceanic tropical convergence zone
ITCZ	Inter tropical convergence zone
ENSO	El Nino Southern Oscillation
RMM	Real-time Multivariate MJO indices
PC	Principal component
EOF	Empirical orthogonal function

1 Introduction

Asian monsoon and El Nino Southern Oscillation (ENSO) are two of the most important components of the tropical coupled ocean–atmosphere system. The tropical temporal climate variability is controlled by life cycles of these large scale climate systems, which also interact with each other. For example, the Asian monsoon is a part of strong annual tropical cycle. On the other hand the main source of tropical interannual variability is ENSO. Both monsoon and ENSO are also mutually and inversely related through large scale convective and circulation patterns in the atmosphere. Another important type of tropical climate variability is in the sub seasonal times scales known as the intraseasonal variability (Gadgil 2003; Webster et al. 1998; Wheeler and McBride 2005). The Madden–Julian oscillation (MJO) is one of the dominant modes of tropical variability on intraseasonal time scales (Madden and Julian 1972). It is a naturally occurring component of the coupled ocean–atmosphere system. It has significant effect on the atmospheric circulation throughout the global Tropics. The MJO can be characterized by large-scale convective anomalies that develop over the tropical Indian Ocean and propagate eastward over the maritime continent to the western Pacific typically in the time scales between 30 and 60 days (Knutson and Weickmann 1987; Hendon and Salby 1994). Large-scale pressure and circulation anomalies develop associated with the convective anomalies. Comprehensive reviews of MJO can be seen in Madden and Julian (1994) and Zhang (2005). MJO is also found to cause variations in weather in even far away extra tropical locations around the globe (Jones 2000; Bond and Vecchi 2003; Carvalho et al. 2004; Barlow et al. 2005; Donald et al. 2006). Recently Wheeler et al. (2009) observed MJO impact on the rainfall and circulation over both tropical and extra tropical regions of Australia during all the four seasons.

The Indian summer monsoon exhibits pronounced intraseasonal variability on timescales ranging from a few days to more than a month (Ramage 1971). The variations in the time scales below 10 days are caused by the synoptic disturbances. However, the most characteristic feature of the intraseasonal variability of the monsoon is the prolonged spells of dry and wet conditions with periodicity of 10–90 days (Goswami 2005). Within this broad range, two prominent oscillations with periodicities in the MJO scale (Raghavan et al. 1975; Yasunari 1979, 1980, 1981; Krishnamurti and Subrahmanyam 1982; Lau and Chan 1986; Gadgil and Asha 1992) and 10–20 days (Murakami 1976; Krishnamurti and Bhalme 1976) respectively have been identified. Spectral peaks in the MJO time scales have also been identified in various other climate parameters over the monsoon region (e.g., Yasunari 1979 (cloudiness), Cadet 1986 (precipitable water), Knutson et al. 1986 (OLR and zonal wind), Krishnamurti et al. 1988 (latent heat flux)). The 10–20 days represent westward propagating mode (Krishnamurti and Ardunay 1980).

The intervals of dry monsoon conditions during which the large-scale rainfall over the monsoon trough zone (the zone between which the monsoon trough fluctuates north and south wards) is interrupted for several days in the peak monsoon months of July and August are known as the breaks (Ramamurthy 1969; Raghavan 1973; Krishnamurti and Bhalme 1976; Alexander et al. 1978). The intervals between spells of dry monsoon conditions when the rainfall is higher than normal are known as active spells. Although interruption of monsoon rainfall was recognized as the most important feature of the break, the first and most recognized criterion for identifying a break was based on the synoptic situation associated with such a rainfall anomaly, rather than the rainfall distribution itself (Ramamurthy 1969). Later there have been several studies that defined monsoon break based on rainfall over India (Rodwell 1997; Annamalai and Slingo 2001; Mandke et al. 2007; Krishnamurthy and Shukla 2000, 2007, 2008; Gadgil and Joseph 2003; Rajeevan et al. 2006, 2008). Recently, Rajeevan et al. (2006, 2008) suggested criteria for identification of active and break events of the Indian summer monsoon on the basis of average rainfall over a critical area over central India, called the core monsoon zone. Active and break events were defined as periods in which the normalized anomaly of the rainfall over the monsoon zone exceeds 1 or is less than -1.0 respectively, provided the criterion is satisfied for at least three consecutive days. Figure 1 shows the normalized daily rainfall anomalies averaged over monsoon zone region for the 2008 southwest monsoon season. The Fig. 1 clearly brings out the intraseasonal variation in the monsoon rainfall with short period break and active spells during July and August. In association with break and active Phases of contrasting rainfall conditions over monsoon zone, the pressure and circulation patterns over Indian region also show contrasting features.

Understanding and predicting of the break and active events have been of great interest because of its impact

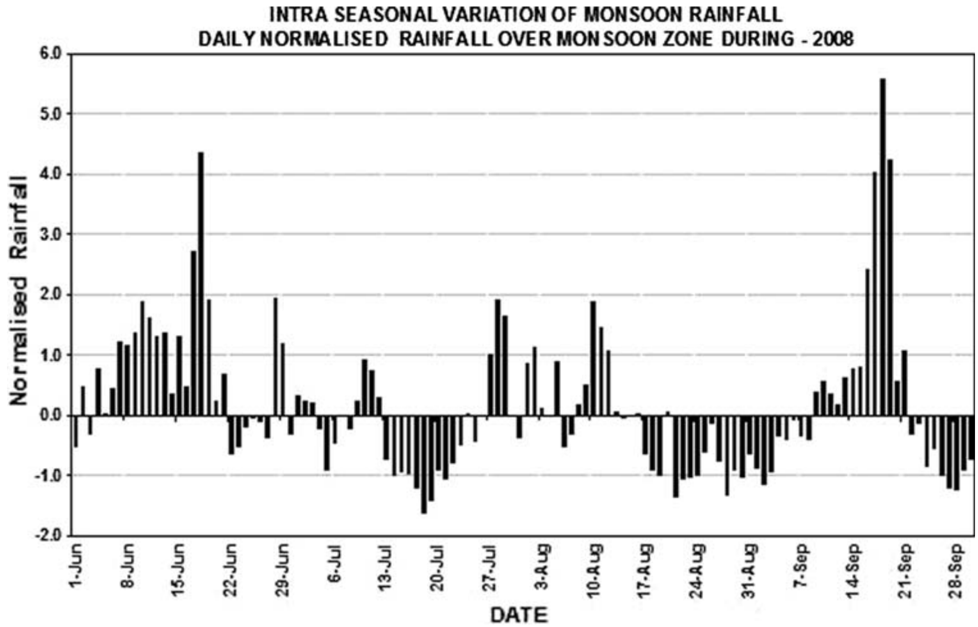

Fig. 1 Daily normalized rainfall anomaly over monsoon zone region for the 2008 monsoon season

on the total seasonal rainfall. Prolonged breaks during a season can lead to deficient monsoon season. The timing of break and active events has also sociological importance and it is particularly relevant for farmers and water managers. Prolonged breaks at critical life stages adversely affect crop development and growth, and hence yield (Lal et al. 1999; Gadgil et al. 1999; Webster and Hoyos 2004). Gadgil et al. (1999) showed that the Indian ground nut production is profoundly influenced by the break monsoon conditions. The availability of the forecasts in the intraseasonal time scales can even help in the decision making in the agriculture such as scheduling of planting and harvest operations, maintenance works, the application of fertilizer etc. (Meinke and Stone 2005).

The main objective of this study was to examine the impact of MJO on the intra seasonal variation in the southwest monsoon rainfall over India by analyzing the rainfall anomaly distribution over India during different Phases of the MJO evolution. The changes in the convective and the lower tropospheric circulation over the Indo-Pacific region associated with the various Phases of the MJO life cycle were used to explain the impact of the MJO on the observed changes in the rainfall distribution over India. The break and active monsoon events during the data period were also analyzed with MJO evolution in the back ground to identify the preferable MJO Phases for onset of these events and its impact on the duration of the events.

The details of the data used and their sources are described in the Sect. 2. The methodology of the study is explained in the Sect. 3. The results of the study are presented in the Sect. 4 and the summary and conclusions of the study are finally given in the Sect. 5.

2 Details of data used

The Real-time Multivariate MJO indices (RMM1 and RMM2) of Wheeler and Hendon (2004) were used for defining the various Phases of MJO. The data were obtained from http://www.bom.gov.au/bmrc/clfor/cfstaff/matw/maproom/RMM/. MJO indices were calculated as the principal component (PC) time series of the two leading empirical orthogonal functions (EOFs) of combined daily mean fields of 850-hPa and 200-hPa zonal winds and OLR averaged over the tropics (15°S–15°N). The annual cycle and the low-frequency variability associated with ENSO were subtracted before calculating the EOFs. These indices are useful in viewing the MJO in a way that is reminiscent of the original schematic of Madden and Julian (1972), comprising convectively-coupled, vertically oriented circulation cells that propagate eastward around the globe along the equator. Wheeler and Hendon (2004) suggested a two dimensional Phase–space diagram with RMM1 and RMM2 as the horizontal and vertical Cartesian axes respectively for viewing the evolution of the MJO. The Phase–space can be divided into eight equal sectors representing eight Phases of MJO evolution. Each of these Phases represents approximate location of the MJO's convective envelope around the global tropics. Phases 2 and 3 correspond to period when the MJO's convective envelope is in the equatorial Indian Ocean, and Phases 6 and 7 correspond to the period when it is in the equatorial Pacific

Ocean. When the amplitude $\left(\sqrt{\mathrm{RMM1}^2 + \mathrm{RMM2}^2}\right)$ is ≥ 1, these eight Phases are categorized as "strong" MJO Phases. When the amplitude is less than one, irrespective of the Phase of the MJO, the MJO is categorized as "weak". Thus in this Phase–space diagram, MJO was categorized in to eight "strong" MJO Phases and a "weak MJO" category. The Phase–space diagram has been used in this study for preparing Figs. 4, 5, 6, 7 and 10. Encircled numbers (1–8) has been used in the diagram to indicate the eight Phases. The unit radius circle with its center at origin of the Phase–space diagram delineates the strong and weak MJO categories.

Another important data set used for this study was the India Meteorological Department (IMD) high resolution gridded daily rainfall data over Indian land region. The original data set was developed by Rajeevan et al. (2006) for the period 1951–2003 using 1,803 stations. Rajeevan et al. (2008) later recalculated the grid point values for the period 1951–2007 using the same technique as Rajeevan et al. (2006) but using 2,140 stations. For interpolating daily station rainfall data into grids of 1° × 1° resolution, Shepard (1968) interpolation method was used. The standard quality controls were applied on the station rainfall data before the interpolation. The interpolated values were computed as the weighted sum of the station data within a search radius of 2.0°. The interpolation is restricted to the radius of influence. The method proposed by Shepard (1968) was used to locally modify the scheme for including the directional effects and barriers. For this study, the data were further extended to 2008.

For examining the impact of MJO on the lower tropospheric circulation, daily 850 hPa wind vector data derived from the National Centers for Environmental Prediction/National Center for Atmospheric Research (NCEP/NCAR) reanalysis (Kalnay et al. 1996; Kistler et al. 2001) were used. The MJO associated changes in the convective patterns were examined using the daily interpolated outgoing longwave radiation (OLR) data measured from Advanced High Resolution Radiometers (AVHRR) aboard NOAA polar orbiting satellites (Liebmann and Smith 1996) as the proxy for the deep convection. Both the wind vector and OLR data sets are available on a 2.5° grid and were obtained from the website of Climate Diagnostics Centre (http://www.cdc.noaa.gov/).

The OLR data were available from June 1974 to September 2008 with missing data during 17 March 1978 to 31 December 1978. As the OLR data is one of the basic components used for computing the MJO indices, the indices values were also available for the same period. All other datasets used were also available throughout this period. Therefore all the data (at daily resolution) for the monsoon season for the period 1974–2008 (except 1978 when OLR data were not available) were used for this study.

3 Methodology

First the daily intraseasonal anomalies of all the fields (rainfall, 850 hPa wind vector, OLR etc.) were computed by subtracting the daily climatology from the daily actual value. The daily climatology was computed as the average of all the daily values for the all the 122 days of the monsoon season (June–September) for the data period of 1975–2007). Thus for each of the field at a grid point, the daily climatology is a single value. For examining the intraseasonal variation in the rainfall distribution during various Phases of MJO evolution, composite daily rainfall maps were prepared for each of the nine categories of MJO (eight strong Phases and one weak MJO category). In order to examine the corresponding changes in the circulation and convective anomalies, composite maps of daily 850 hPa wind vector anomalies and OLR anomalies were also prepared for the all the nine categories of the MJO. Physical mechanism behind the impact of MJO on the intraseasonal variation in the rainfall distribution was explained by relating the changes in the circulation and convective anomalies with the changes in the rainfall distribution. Finally the impact of MJO on the onset of the break and active monsoon events and duration of these events were examined by viewing the MJO evolution in the two dimensional (RMM1, RMM2) Phase diagram during the period of these events.

4 Results

4.1 Intraseasonal variation in the rainfall anomalies over India during different phases of the MJO

During the 34 monsoon seasons of the analysis period (1974 to 2008 except 1978) of this study, the number of

Table 1 Number of days under various MJO Phases for both strong and weak MJO categories during the period 1975–2008 (excluding 1978)

MJO Phase	Number of days for strong (weak) MJO category
1	430 (284)
2	385 (304)
3	214 (229)
4	237 (244)
5	376 (171)
6	307 (174)
7	195 (178)
8	223 (197)
Total	4,148 (1781)

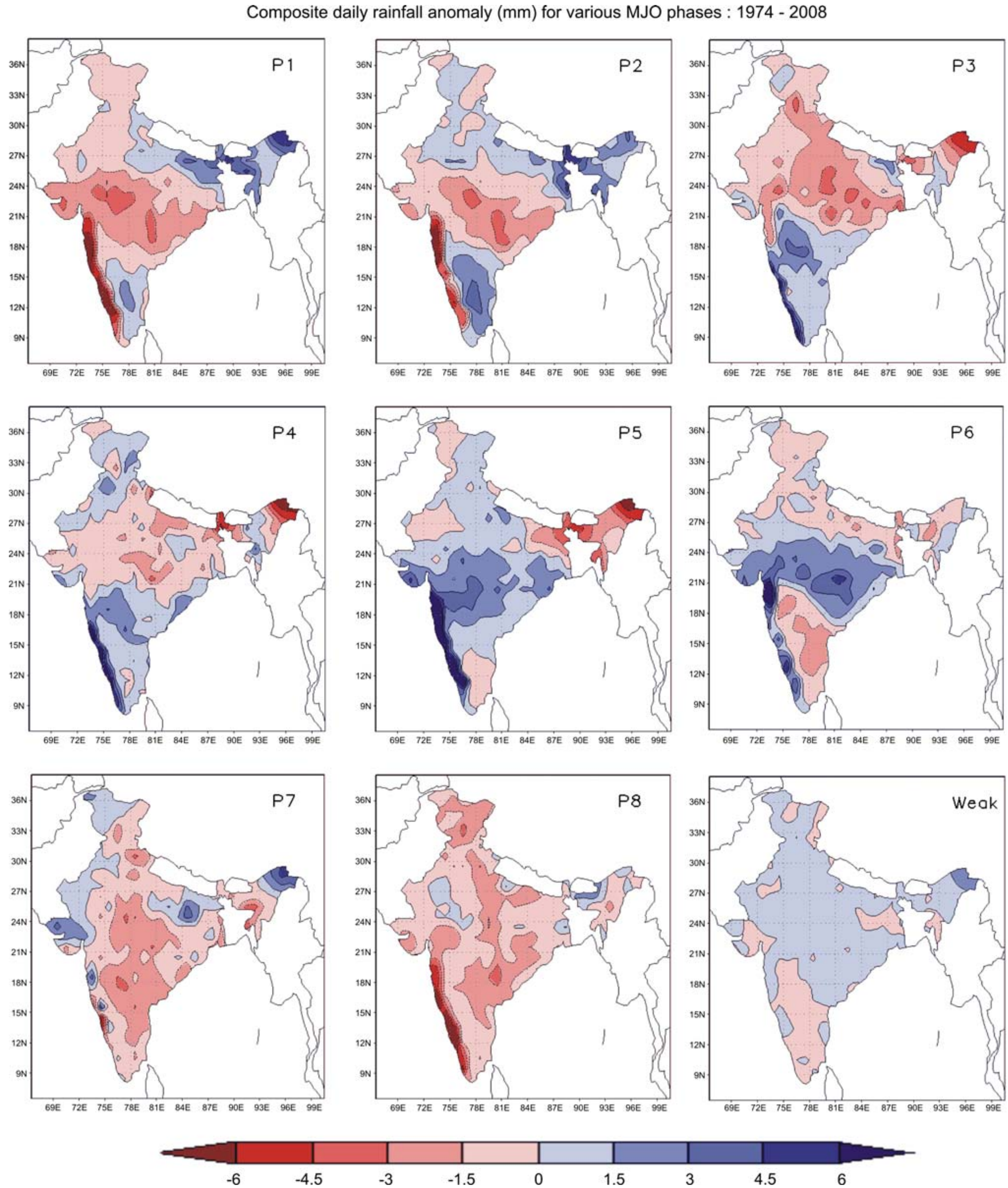

Fig. 2 Maps of composite rainfall anomaly (mm) in respect of eight strong phases and the weak category of MJO derived using data for the period 1974–2008 (excluding 1978). Maps for the eight strong MJO Phases are labeled as 'P1', 'P2' etc. and the map for weak category is labeled as 'weak'

days under each of the eight strong MJO Phases varied from 195 days for Phase 7 to 430 days for Phase 1 (Table 1). There were 1,781 days of the Weak MJO category. Figure 2 shows the composite maps of daily rainfall anomaly for the different 9 categories of the MJO.

During the Phase 1, the rainfall anomalies were negative over monsoon trough zone region and along the entire west coast. The anomalies were positive along the foot hills of the Himalayas, northeast India and southeast India. As a whole the rainfall anomaly pattern during the Phase 1 of MJO resembled to the rainfall pattern associated with the break monsoon condition (Fig. 8a of Rajeevan et al. 2008). During Phase 2, the rainfall anomaly pattern was nearly similar to that of Phase 1 but for noticeable changes in the strength of the anomalies. The most significant changes were the appearance of positive rainfall anomalies over the southern most part of the Peninsula, weakening of negative anomalies over monsoon trough zone and west coast (particularly in the southern side) and strengthening of the positive anomalies over southeast India. This indicated increased rainfall activity during Phase 2 compared to the Phase 1. During Phase 3, the positive anomalies over southeast India spread towards north and west to cover most of the region south of about 20°N. Along most of west coast, the rainfall anomalies were positive. Similarly the negative anomalies over central India were also strengthened and spread to cover most of the region north of 20°N except over some parts of north and northeast of the country, where the anomalies were positive. Thus during Phase 3, the country was nearly divided into two halves of opposite rainfall anomalies with positive anomalies over southern part and negative anomalies over northern part. In Phase 4, the rainfall anomaly pattern was almost similar to that during Phase 3 but with weakened negative anomalies over north India and strengthened positive anomalies over west coast. The positive anomalies over Peninsula also showed slight northward shift, which was more prominent in the eastern part. During Phase 5, the positive anomalies over Peninsular India showed further northward shift and spread over most of central India and some parts of north India. The anomalies over large strip of the west coast were strengthened and showed significant northward shift. Strong negative rainfall anomalies were observed over northeast India and weak negative anomalies were seen over southeast India. During Phase 6, Positive anomalies were observed over monsoon trough zone region and west coast and negative anomalies were observed along the foot hills of Himalayas, northeast India and southeast India. The positive anomalies over monsoon trough zone were stronger and that over west coast were weaker compared to the anomalies observed during previous Phase of MJO (Phase 5). Overall, the rainfall anomaly pattern during Phase 6 was nearly opposite to that during Phase 1 and resembled to the rainfall anomaly pattern associated with the active monsoon conditions (Fig. 8b of Rajeevan et al. 2008). During the subsequent Phase (Phase 7) of MJO, the rainfall anomaly pattern showed sudden changes. Over most parts of the country negative anomalies were seen with positive anomalies only over northwestern most part of the country and some parts of the north, northeast and west coast of the country. Thus the rainfall pattern indicates decreased rainfall over larger scale covering almost all part of the country. The decrease was particularly highest over central India. During Phase 8, most areas of the country except some pockets over northwest and northeast parts showed negative rainfall anomalies with the anomalies over west coast showing more strengthening. During the weak category of (amplitude less than 1) MJO, the composite rainfall anomalies in general were weak as the composite for this category was prepared based on days with all the eight Phases.

From the above results, it is clear that during its life cycle, MJO favoured weakening of the monsoon during the first two and last two Phases and strengthening of the monsoon during the four intermediate Phases the MJO. The transition from weak monsoon during Phases 1 and 2 to that representing strong monsoon during Phases 5 and 6 was relatively slow and systematic compared to the rapid changes observed in the opposite direction from Phases 5 and 6 to Phases 7 and 8. It may be mentioned that the duration of the active monsoon events are in general smaller compared to that of break events (Rajeevan et al. 2008).

4.2 Composite OLR and 850 hpa wind vector anomalies over Asia-Pacific region

In the earlier section, changes in the rainfall anomaly patterns associated to various Phases of MJO were examined. Now we examine how these changes are related to the changes in the lower tropospheric circulation and convective anomalies over Asia-Pacific region. Figure 3 shows the composite of daily OLR anomalies superposed with composite 850 hPa wind vector anomalies for the different Phases of the MJO. The formation of MJO starts in the Phase 1 with a zone of negative OLR anomalies indicating above normal convection appearing throughout the equatorial Indian Ocean with maximum anomalies along the zone just south of the equator indicating active oceanic tropical convergence zone (OTCZ). OLR anomalies of opposite sign were seen over the monsoon trough region which extended south eastwards over northwest Pacific up to date line indicating suppressed convection along the northern hemisphere inter tropical convergence zone (ITCZ). De et al. (1995) have shown inverse relationship between the activity of the OTCZ and rainfall over central

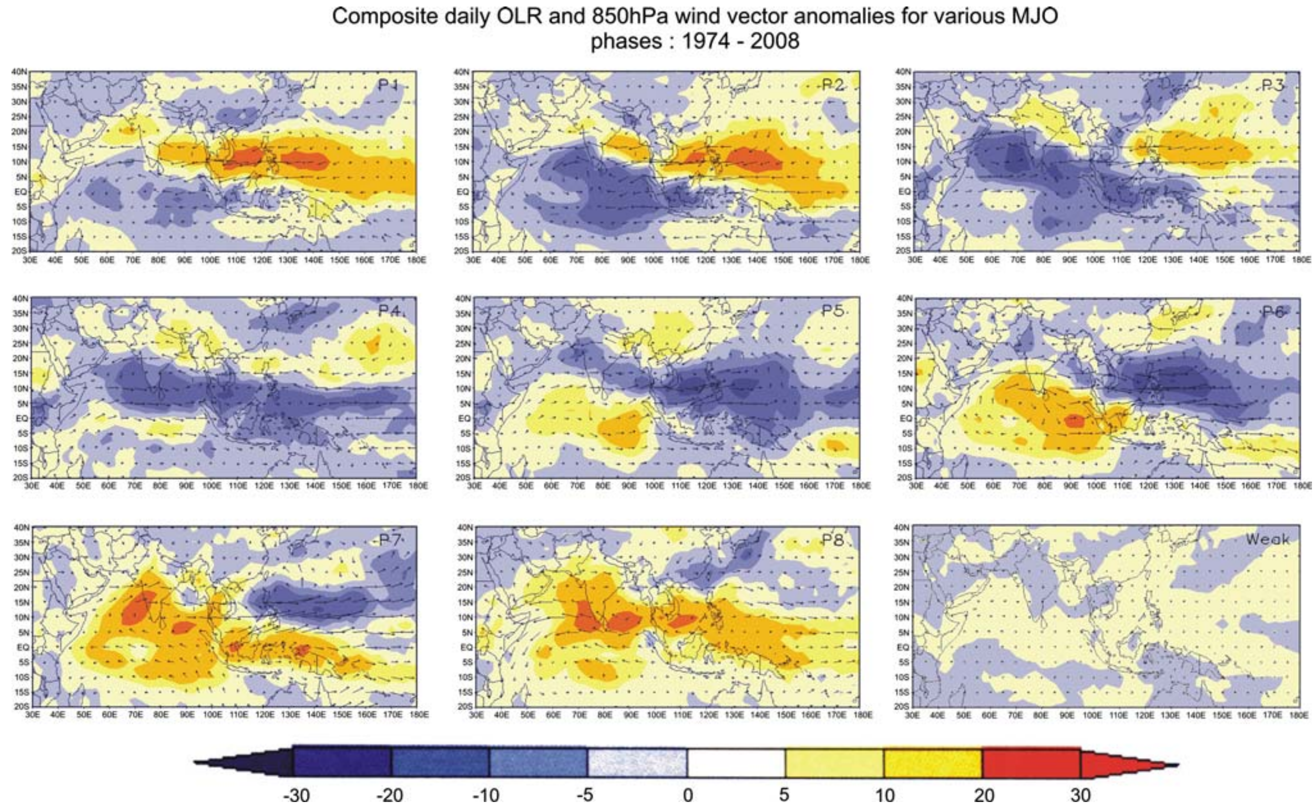

Fig. 3 Maps of composite daily OLR anomaly (W m^{-2}) superposed with composite 850 hPa wind vector anomaly in respect of eight strong phases and the weak category of MJO derived using data for the period 1974–2008 (excluding 1978). Maps for the eight strong MJO Phases are labeled as 'P1', 'P2' etc. and the map for weak category is labeled as 'weak'

India. The OLR anomalies of opposite signs over ITCZ and OTCZ formed a dipole like pattern. A similar dipole pattern was observed by Goswami and Ajayamohan (2001) in the composite precipitation anomalies over Asia Pacific region associated with the break monsoon conditions. RameshKumar et al. (2009) observed that the above normal convection over equatorial Indian Ocean is an important feature associated with breaks and due to the increasing trend in the convective activity over this region in recent decades, the frequency of breaks have also shown an increasing trend. The 850 hPa wind vector anomalies were complimentary to OLR anomalies with easterly or northeasterly anomalies observed south of 15°N over region extending from northwest Indian Ocean to northwest Pacific. A feeble anomalous cyclonic circulation was observed just close to equator about 70°E. Anomalous ridge from the center of an anomalous anticyclonic circulation over monsoon trough zone extended eastwards to the center of another anomalous anticyclonic circulation over northwest Pacific.

During Phase 2, the convective and the circulation anomaly patterns were nearly same as that during Phase 1 except for a northward shift by about 5° and some changes in the magnitude and spatial extension of the anomalies. The zone of maximum in the negative OLR anomalies over north equatorial Indian Ocean was oriented southeast to northwest extended from equator to about 15°N. During Phase 3, this zone of maximum negative OLR anomalies and associated anomalous cyclonic circulation anomalies showed further northeastward shift by about 5°. The westerly anomalies south of this cyclonic circulation anomaly helped strengthening of the cross equatorial flow in the south Arabian Sea and increasing rainfall activity over south Peninsula as a whole and over west coast in particular as seen in the Fig. 2.

During Phase 4, with the entry of the MJO into the maritime continent region the eastern part of the ICTZ showed strengthening. The zone of negative OLR anomalies extended from Arabian Sea to date line. Over Indian region the convective and circulation anomalies indicated, the transformation of OTCZ to monsoon trough. At the same time, positive OLR anomalies were seen along most of equatorial Indian Ocean. Thus at this stage, the impact of MJO on the ITCZ was to enhance convection along ITCZ through its direct and indirect influence. The enhancement of convection in the eastern part of ITCZ over west Pacific by the positive convective anomalies associated with the eastward propagating MJO is the direct influence. The enhancement of convection in the western part of the ICTZ (over monsoon trough over India) by the northward propagating positive convective anomalies activated by MJO during its Phases 1 and 2 is the indirect influence.

In the Phase 5, the entire ITCZ showed north ward shift. Over India, the monsoon trough (part of ITCZ) showed maximum shift with the western part showing a shift of about 10° and eastern part showing a shift of about 5°. On either side (south and north) of the monsoon trough, the OLR anomalies were positive. In the south, along the equatorial region sudden change in the convective anomaly pattern was clearly visible. The large dipole like pattern in the convective pattern observed during the first three Phases of MJO was now suddenly reversed with MJO close to west Pacific as reflected by the expanded areas of strong negative OLR anomalies over west Pacific. This transition was however initiated during Phase 4 and the reversed dipole structure in the OLR anomaly was observed till Phase 6. The northward extension of southwesterly anomalies over Arabian Sea also indicated strengthening of the cross equatorial flow. All these features were helpful for increased rainfall activity over most parts of the country except northeast India as reflected in the rainfall anomaly pattern.

During Phase 6, with MJO active in the Pacific, the positive OLR anomalies over equatorial Indian Ocean and negative OLR anomalies over west Pacific were further strengthened. Corresponding changes were also observed in the 850 wind anomaly pattern with anomalous cyclonic circulation over west Pacific and anticyclonic circulation anomaly over equatorial Indian Ocean. Over Indian region, anomalous trough along with negative OLR anomalies was observed over the monsoon trough zone. The cross equatorial flow across Arabian Sea was further strengthened. All these features provided active monsoon conditions over India as indicated by the rainfall anomalies during Phase 6.

During the subsequent two Phases of MJO, with the negative OLR anomalies over Indian monsoon region shifting further northward and that over northwest Pacific shifting further eastward (in association with the eastward propagation of MJO), the entire ITCZ became weaker than normal. As a result, the positive OLR anomalies over equatorial Indian Ocean were seen spreading northward over nearly entire Indian monsoon region and eastward over maritime continent region and west Pacific. In the lower troposphere, during Phase 7, an anomalous anticyclonic circulation was observed over south Peninsula with strong westerly anomalies over north India and easterly anomalies over eastern equatorial Indian Ocean. During Phase 8, this anomalous anticyclonic circulation was further shifted to north resulting in the appearance of northeasterlies over Arabian Sea. This resulted in the weakening of cross equatorial flow and further decrease in the rainfall activity.

For weak MJO category (last anomaly map in the Fig. 3), as expected the OLR and 850 hPa wind vector anomalies were very weak though the OLR anomalies were negative over most parts of the country.

On comparing the OLR anomaly patterns of Phases 8 and 1, it can be seen that OLR anomaly pattern during Phase 8 nearly resembled to that of Phase 1 except for the negative OLR anomalies over equatorial Indian Ocean. So it is very clear that if another MJO linked positive convective anomalies forms over Indian Ocean, the convective anomaly pattern corresponding to Phase 8 can quickly change to that observed during Phase 1 and another cycle of changes in the convective and circulation anomaly patterns as observed in the Fig. 3 can take place and the rainfall pattern over India can experience another cycle of intraseasonal oscillation.

4.3 Relationship between break and active monsoon events over India and MJO Phases

To examine the association of the break and active events with the various Phases of MJO, the break and active events for the period 1974–2007 were considered from the list of these events provided for the period 1951–2007 in Rajeevan et al. (2008). In addition, the break and active events for 2008 were derived using the criteria of Rajeevan et al. (2008). During 2008 (see Fig. 1), the periods of 14–19 July and 21–24 August were identified as the break events and periods of 27–29 July and 10–12 August were identified as active events. During the period 1974–2008 (excluding 1978), there were 47 break events (265 break days) and 57 active events (237 active days). In order to identify the most preferable phases of MJO for the onset of break and active monsoon events, MJO index values corresponding to onset day of these events were plotted in the (RMM1, RMM2) Phase diagram. The Fig. 4 depicts the Phase diagram for break events. Different markers have been used in the Phase diagram to distinguish between break events of duration of <6 days, 6–9 days and ≥10 days. In addition, events of duration ≥10 days have been shown with labels indicating their duration. For example, the label 14-29A79 means the break event of duration 14–29, August, 1979. It can be seen from Fig. 4 that onset day of majority of the break events (39 of the total 47 break events (83%) associated with the Phases 7, 8, 1 and 2 with maximum during Phase 1 (40%). Similarly onset day of 16 of the 19 break events (84%) of the duration of ≥6 days (both events of duration 6–9 days and ≥10 days together) were associated with these four Phases with maximum (8 events) during Phase 1 (42%). Another important point is that all of the four long duration break events (≥10 days) were set in during the Phases 7 and 8 (one event initiated just in the boundary between Phases 8 and 1). However, once the MJO entered into east equatorial

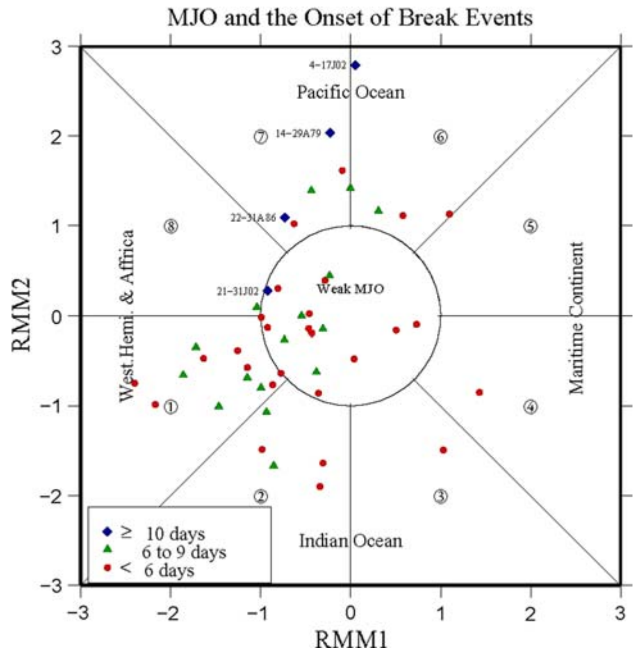

Fig. 4 The Phase–space diagram depicting MJO indices for the first day of the 47 break events occurred during the period 1974–2008 (excluding 1978). The encircled numbers inside eight sectors of the diagram represent eight phases of the MJO in the diagram. The circle of unit radius with centre at the origin of the diagram delineates the strong and weak MJO categories. Break events of duration <6 days, 6–9 days and ≥10 days are shown using distinct markers. In addition, labels indicating the duration of the events are shown near to the markers corresponding to the events of duration ≥10 days. For example, the label 14-29A79 represents the break event of duration 14–29, August, 1979

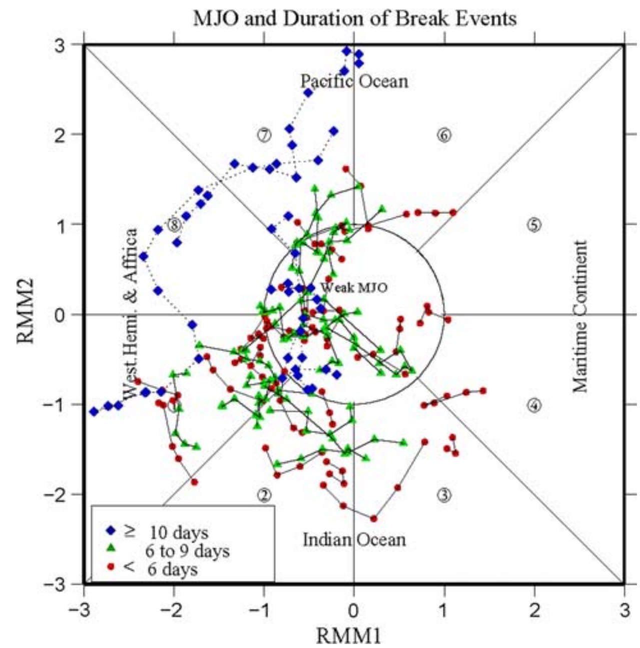

Fig. 5 The daily MJO indices plotted using markers during the entire duration of each of the 47 break events occurred during the period 1974–2008 (excluding 1978). The *encircled numbers* inside eight sectors of the diagram represent eight phases of the MJO in the diagram. The circle of unit radius with centre at the origin of the diagram delineates the strong and weak MJO categories. Break events of duration <6 days, 6–9 days and ≥10 days are shown using *distinct markers*. Markers corresponding to each of the break events of duration <6 days and 6–9 days are connected with *solid lines* separately and that of duration ≥10 days are connected with *dotted lines*

Indian Ocean and till it entered into west Pacific (Phases 3 to 6), very few break events were initiated.

In order to examine the impact of the MJO on the duration of the break events, the daily MJO indices corresponding to each of the break events were plotted in the (RMM1, RMM2) Phase diagram (Fig. 5) and were joined with lines so that their length will reflect the duration of the events. Just like in the Fig. 4, the events of duration of <6 days, 6–9 days and ≥10 days have been distinctly depicted. In general, the markers in the anti-clock wise direction along each of the curves represent approximate daily location of the east ward propagating MJO during that event. The most significant point that inferred from Fig. 5 is that, though the maximum number of breaks gets set in during the Phase 1, these events do not prolong. On the other hand, the break events set in when the MJO were strong and located in the Pacific (Phases 7 and 8) have better chance to prolong for longer duration. Another significant point is that most of the break events came to end by the time MJO started propagating over Maritime continent and nearly no break events existed when the MJO was located the eastern parts of maritime continent (Phase 5).

Figures 6 and 7 are same as Figs. 4 and 5 but for the active monsoon case. From the Fig. 6, it is seen that onset of the active events have taken place during all the Phases of MJO. But 40 of the 57 active events (70%) were set in during the four MJO Phases of 3 to 6 with maximum during Phase 4 (21%). Further, 7 of the 9 active events (78%) of duration of ≥6 days (both events of duration 6–9 days and ≥10 days together) were initiated during Phases 4 and 5 and remaining 2 active events were initiated during Phase 1. There was only one active event of duration of ≥10 days (13–22, August 06) which was initiated during Phase 5. Thus when the MJO was located between east equatorial Indian Ocean to west Pacific, the possibility for onset of active events was relatively higher. However, the important point to be noted is that 4 of 9 active events of duration of ≥6 days including the longest duration were set in during the weak MJO category. In fact, 27 of the 57 active events (47%) were set in during the weak MJO category. This is a major difference with break case as onset of most of the break events (33 of the 47 events (70%)) were during strong Phases of MJO and only 14 break events (30%) were set in during the weak MJO.

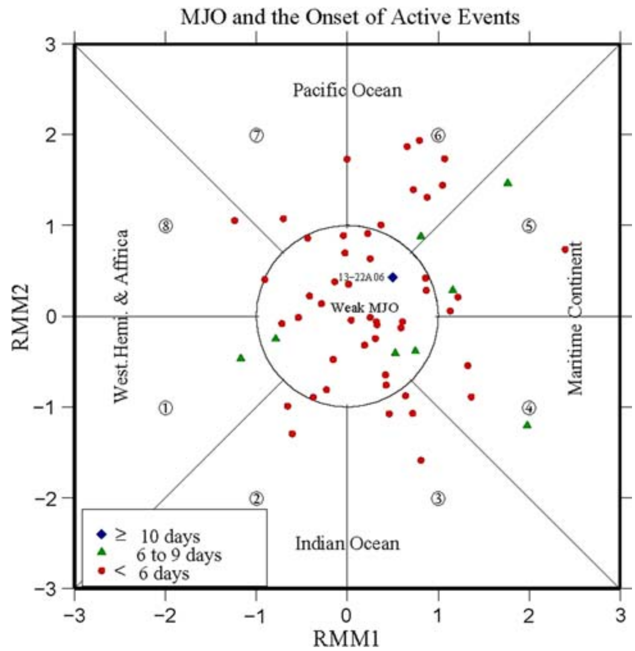

Fig. 6 Same as Fig. 4. But for the 57 active events occurred during the period 1974–2008 (excluding 1978)

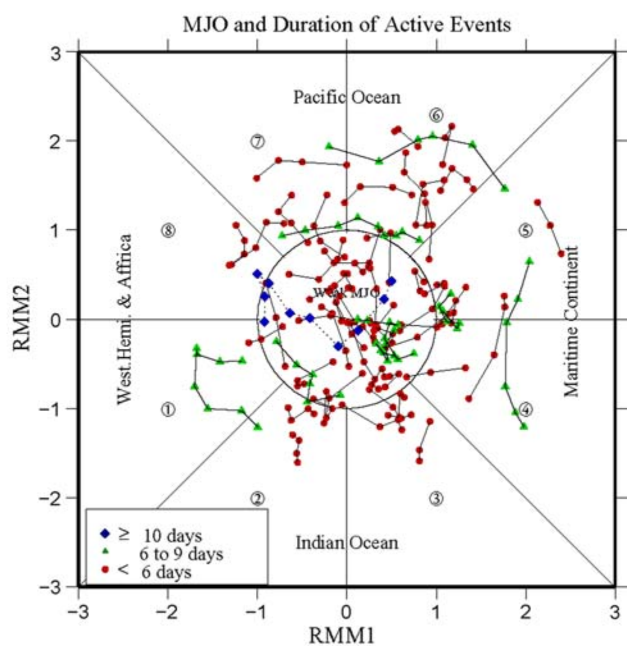

Fig. 7 Same as Fig. 5. But for the 57 active events occurred during the period 1974–2008 (excluding 1978)

Further, as described earlier in this section, onset of break events has strong preference to certain Phases of MJO (Phases 1, 2, 7 and 8). Whereas the onset of active events though has some preference to the Phases 3 to 6, it has occurred during all the Phases. As seen in Fig. 7, the end of active events also did not show preference for any particular MJO Phases and entire duration of many of the active events have totally occurred during the weak Phases.

More critical examination of break and active events revealed that 109 of the 265 break days (41%) and 113 of the 237 active days (48%) were in the weak MJO category. The Fig. 8 depicts the frequency distribution of the break days during the eight Phases of MJO for both strong and weak categories. It can be seen that when the MJO is strong, maximum number of break days were associated with the Phase 1 followed by Phase 2. For the weak MJO category also, the maximum number of break days were associated with the Phase 1. However, for the weak MJO category, the sum of the number of break days during Phases 7 and 8 was nearly equal to that during Phases 1 and 2. Thus on considering all the 265 break days irrespective of the strength of the MJO, the maximum number of break days (86%) were associated with the first two (Phases 1 and 2) and the last two (Phases 7 and 8) Phases.

Figure 9 is same as Fig. 8 but for active days. As seen in the Fig. 9, 124 active monsoon days were associated with the eight strong MJO Phases with maximum frequency during the Phases 5 and 6. However, within the active days associated with weak MJO category, the maximum frequency was during the Phase 4 followed by Phase 3. Both strong and weak categories taken together, relatively highest number of active days (62%) were associated with the four Phases from Phase 3 to Phase 6.

Thus the results of this section suggest that the onset and duration of break and active events were related to the strength and Phase of MJO. However, the association of break monsoon events with MJO was relatively stronger than the association of active events with MJO.

5 Summary and conclusions

The composite rainfall anomaly analysis associated with the various Phases of MJO revealed strong intraseasonal variation in the spatial rainfall anomaly distribution over India. During MJO Phases of 1 and 2, break monsoon type rainfall distribution was observed over India. Subsequently, as the MJO propagated eastwards, a gradual northward shift of the above normal rainfall band from south Peninsula to north India was observed. During Phases 5 and 6, the above normal rainfall band was observed along monsoon trough region and active monsoon type rainfall distribution was observed. During the subsequent Phases (7 and 8) a general decrease in the rainfall was observed over most parts of the country. The observed intraseasonal variation in the rainfall can be explained by the changes in the convective and circulation anomalies observed in association with the formation of MJO induced positive convective anomalies over equatorial Indian Ocean during

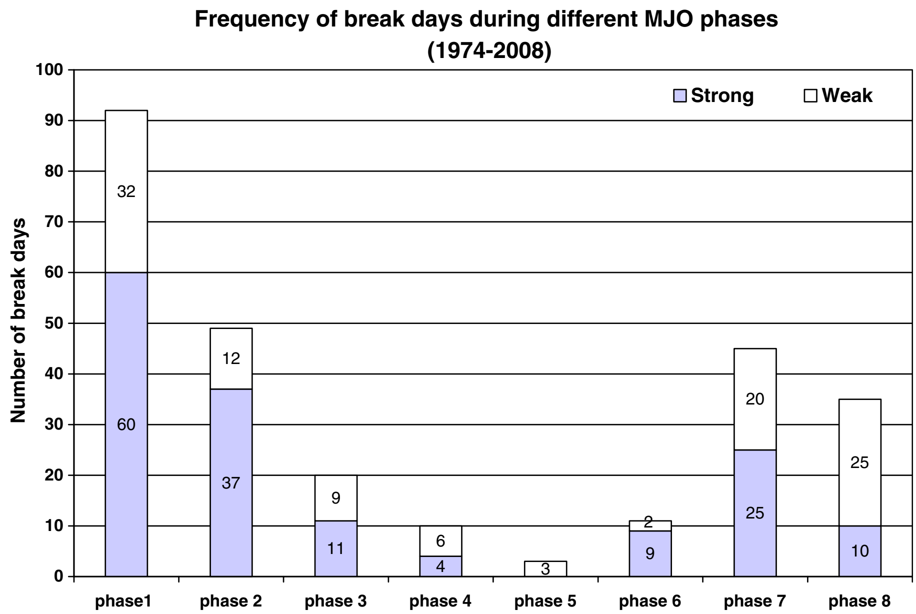

Fig. 8 Bar diagram representing frequency distribution of break days for the various Phases of MJO for both strong and weak categories

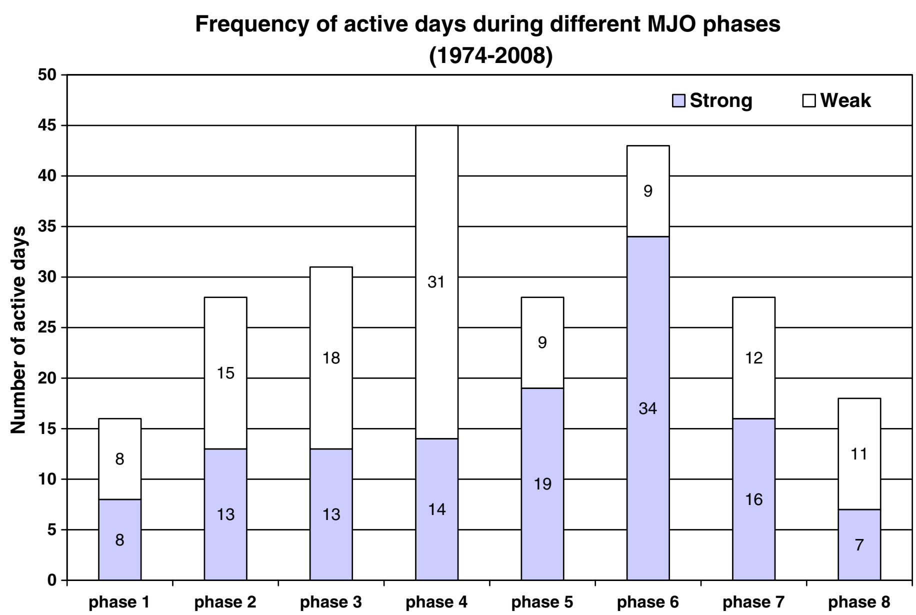

Fig. 9 Bar diagram representing frequency distribution of active days for the various Phases of MJO for both strong and weak categories

Phases 1 and 2 and its northward propagation. Earlier studies have also reported northward propagation of cloud bands/rainfall anomalies over Indian monsoon region with MJO periodicity (Yasunari 1979; Sikka and Gadgil 1980; Singh and Kripalani 1985, 1986; Gadgil et al. 2003).

The MJO induced above normal convection over the equatorial Indian Ocean during Phases 1 and 2 strengthened the OTCZ over the region. The associated anomalous rising motion over the region caused large scale anomalous subsidence over the monsoon trough region as manifested by the low level anomalous anticyclone over the region. These factors weakened the monsoon circulation and resulted in break monsoon type situation. Associated negative convective anomalies over monsoon trough region extended eastwards to date line indicating weaker than normal northern hemisphere ITCZ and formed dipole like pattern with convective anomalies of opposite sign along active OTCZ.

Subsequently, as the MJO propagated eastwards from west equatorial Indian Ocean to west equatorial Pacific through the maritime continent, a gradual northward shift of OTCZ by about 5° per Phase was observed. Around Phase 4 MJO induced OTCZ was transformed as monsoon trough over Indian monsoon region and activated western part of the ITCZ. Meanwhile, the eastward propagating MJO associated convective anomaly activated eastern part of the ICTZ. During Phases 5 and 6, the activated monsoon trough moved northward to its normal position and active monsoon type convective and circulation anomaly patterns were set in. During Phases 5 and 6, the dipole like pattern in the convective anomalies was reversed with negative anomalies over equatorial Indian Ocean and positive anomalies along ITCZ. Associated anomalous subsidence motion over equatorial Indian Ocean and anomalous rising motion over monsoon trough region caused stronger than normal monsoon circulation. Similar changes in the sign of the convective and circulation anomalies across large region extending from Indian monsoon region to equatorial Pacific during various phases of MJO life cycle showed that the impact of the MJO was not limited to Indian region but was experienced over large areas of the Asia-Pacific region.

It may be mentioned that no kind of band pass or other filtering was carried out on the anomalies (of rainfall, OLR and 850 hPa wind vector) used for preparing composite maps presented in this study. However, for confirming robustness of the results, the daily anomalies were band-pass filtered to retain periodicity of 10–90 days using a Lanczos filter (Duchon 1979) and the composites were recalculated. Interestingly, all the recomputed composite maps with filtered anomalies were nearly same as that presented in this study (Figs. 2, 3) except that the magnitudes of the filtered anomalies were lower than the anomalies without filtering.

Another important finding of this study is observed strong impact of MJO on the onset of break and active monsoon events over India and their duration. Though the amplitude of the MJO plays a significant role in this association, the Phase of the MJO seems to be more deciding factor. In general, occurrence of the active events showed relative preference to weak MJO (amplitude less than 1) than the break events. Onset of most of the break events (33 of the 47 events (70%)) were during strong Phases of MJO and only 14 break events (30%) were set in during the weak MJO. Whereas the onset of 48% of the active days were associated with the weak category of MJO and that of only 41% of the break days were associated with the weak MJO. This means weak or absence of MJO activity generally helps normal or active monsoon conditions. Kripalani et al. (2004) showed that MJO scale oscillations were the dominant mode of the intraseasonal variation of monsoon rainfall during the drought monsoon year of 2002 and was weak or absent during the normal monsoon year of 2003.

On considering the Phases of the MJO, onset of about 83% of the break events were during the Phases 7, 8, 1 and 2 with maximum during Phase 1 (40%). Similarly, 86% of the break days were observed associated with these four MJO Phases. Another important point is that the break events set in during the MJO Phases of 7 or 8 has higher probability to prolong. This may be because when the break event is already set in during Phases of 7 or 8 and the MJO re-originate in the India Ocean, the changes in the monsoon circulation associated with Phases 1 and 2 delays the monsoon revival. On the other hand, possibility for onset of active events was relatively higher during the Phases of 3 to 6. About 70% of the active events were initiated during these four MJO Phases with maximum during Phase 4 (21%). Similarly, 62% of the active days were associated with Phases 3 to 6. Thus association of active days to the preferred MJO Phases was weak compared to that of break days with the preferred MJO Phases.

In addition to break and active events, another important intraseasonal phenomenon that can be associated with MJO is the date of Monsoon onset over Kerala (MOK). Figure 10 shows the Phase–space diagram plotted with MJO indices corresponding to the date of MOK during the period 1975 to 2008 (excluding 1978). The dates of MOK used here were derived using new IMD criteria (Pai and Rajeevan 2009). Wheeler and Hendon (2004) have also shown a similar plot but the dates of monsoon onset over Kerala used there was derived based on the earlier criteria used by IMD for declaring monsoon onset over Kerala (Ananthakrishnan et al. 1967). The dates MOK for the

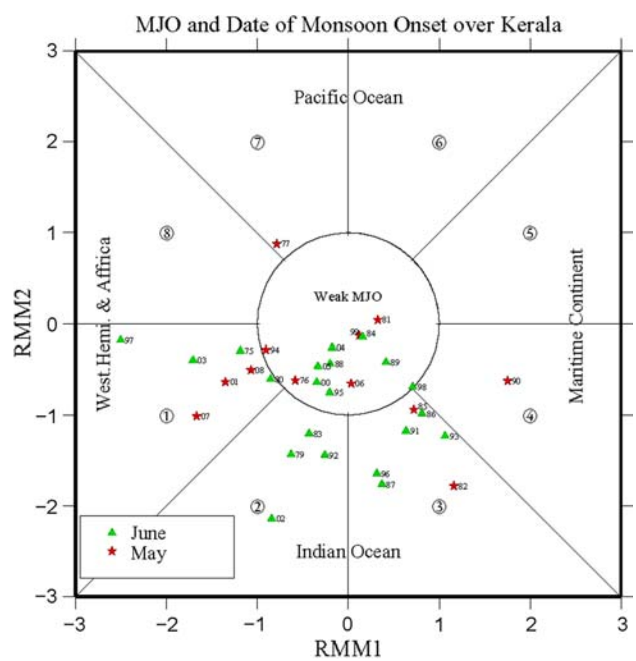

Fig. 10 The Phase–space diagram depicting MJO indices corresponding to the dates of monsoon onset over Kerala for the period 1975–2008 (excluding 1978). Separate markers are used for May and June events. The *encircled numbers* inside eight sectors of the diagram represent eight phases of the MJO in the diagram. The circle of unit radius with centre at the origin of the diagram delineates the strong and weak MJO categories

period 1971–2007 based on both criteria have been given in Pai and Rajeevan (2009). It can be seen that the during 28 of the 33 cases of this period, monsoon onset over Kerala has occurred in associated with the MJO Phases of 1, 2 and 3. Earlier we have seen that during these three phases, positive convective anomalies associated with MJO form over the equatorial Indian Ocean and propagate northward.

It may be noted that the results of the study only indicate the average impact of all the MJO events that occurred during the period of study and which were different from each other in terms of amplitude and time of occurrence. For individual events, the impact may be slightly different from the composite picture. However, the results of this study provide an opportunity to use the real time information of the state of MJO for qualitative prediction of the intraseasonal variability of monsoon rainfall particularly the onset and duration of the break and active events which are very crucial for agriculture decisions. The Wheeler and Hendon (2004) MJO indices (RMM1 and RMM2) used in this study are available in real time. Availability of skillful forecasts of state of MJO on real time will further help towards this cause. Few research centers are already providing on line real time MJO forecasts. Bureau of Meteorological Research Center (BMRC) is providing forecast of forecasts of daily RMM1 and RMM2 values based on time series analysis developed by Maharaj and Wheeler (2005). BMRC is also providing pentad OLR anomalies forecast over global tropics with lead periods of 5–20 days based on seasonally-varying lagged linear regression with RMM1 and RMM2 as predictors recently Jiang et al. (2008). School of Environmental Sciences and School of Mathematics, University of East Anglia, UK (http://envam1.env.uea.ac.uk/mjo.html) is providing real time pentad OLR anomaly forecasts with lead periods of 5–40 days based on empirical techniques (Love et al. 2008) in which MJO signal was extracted from the grid point OLR anomaly data using the empirical mode decomposition and then fed as input to a vector autoregressive moving average (VARMA) model. Earth System Research Laboratory (http://www.cdc.noaa.gov/mjo/Predictions/) is providing near real time MJO forecasts from seven different dynamical and statistical forecasting systems. Over the Indian region, IMD is providing real time pentad OLR anomaly forecasts (www.imdpune.gov.in) with lead periods of 5–20 days using the analog method of Xavier and Goswami (2007). However, Waliser et al. (2006) analyzing various statistical and dynamical models for MJO prediction found that the present skill of the prediction of intraseasonal variation is relatively less compared to the skill levels currently available in short term weather forecasts.

One of the important objectives of the proposed Continental Tropical Convergence Zone (CTCZ) Programme over Indian monsoon region under Indian Climate Research Programme (ICRP 2008) to understand the mechanism leading to space-time variation of the CTCZ over Indian region (monsoon trough) during the monsoon and its relation with the convection over surrounding oceans. The CTCZ programme will involve field experiments over Indian monsoon region using land, ocean and space based observational systems during the period 2009–2012. It will also involve diagnostic studies, data assimilation and modeling studies. Therefore, this programme should help in providing valuable observational and modeling results for the further understanding of the underlying physical mechanism behind break and active spells in monsoon and its prediction.

Acknowledgments We express our sincere thanks to Dr. Ajit Tyagi, DGM, India Meteorological Department for the encouragement and support in carrying out this research work. We also thank Dr. M. Rajeevan and Dr. M. C. Wheeler for their valuable suggestions for the improvement of this manuscript.

References

Alexander G, Keshavamurty RN, De US, Chellappa R, Das SK, Pillai PV (1978) Fluctuations of monsoon activity. Indian J Meteorol Geophys 29:76–87

Ananthakrishnan R, Acharya UR, Ramakrishnan AR (1967) On the criteria for declaring the onset of the southwest monsoon over Kerala. Forecasting Manual. FMU Report No. IV-18.1:52. India Meteorological Department, Pune, India, 1620–1639

Annamalai H, Slingo JM (2001) Active/break cycles: diagnosis of the intraseasonal variability of the Asian Summer Monsoon. Clim Dyn 18:85–102

Barlow M, Wheeler MC, Lyon B, Cullen H (2005) Modulation of daily precipitation over southwest Asia by the Madden-Julian oscillation. Mon Weather Rev 133:3579–3594

Bond NA, Vecchi GA (2003) The influence of the Madden-Julian oscillation on precipitation in Oregon and Washington. Weather Forecast 18:600–613

Cadet DL (1986) Fluctuations of precipitable water over the Indian Ocean during the 1979 summer monsoon. Tellus 38A:170–177

Carvalho LM, Jones C, Liebmann B (2004) The South Atlantic convergence zone: intensity, form, persistence, and relationships with intraseasonal to interannual activity and extreme rainfall. J Clim 17:88–108

De US, Prasad O, Vaidya DV (1995) The influence of the Southern Hemisphere Equatorial Trough on rainfall during the southwest monsoon. Theor Appl Climatol 52:177–181

Donald A, Meinke H, Power B, Maia AHN, Wheeler MC, White N, Stone RC, Ribbe J (2006) Near-global impact of the Madden-Julian oscillation on rainfall. Geophy Res Lett 33:L09704. doi: 10.1029/2005GL025155

Duchon C (1979) Lanczos filtering in one and two dimensions. J Appl Meteorol 18:1016–1022

Gadgil S (2003) The Indian monsoon and its variability. Annu Rev Earth Planet Sci 31:429–467

Gadgil S, Asha G (1992) Intraseasonal variations of the Indian summer monsoon. Part I: observational aspects. J Meteorol Soc Jpn 70:517–527

Gadgil S, Joseph PV (2003) On breaks of the Indian monsoon. Proc Indian Acad Sci Earth Planet Sci 112:529–558

Gadgil S, Seshagiri Rao PR, Sridhar S (1999) Modelling impact of climate variability on rainfed groundnut. Curr Sci 76:557–569
Gadgil S, Vinayachandran PN, Francis PA (2003) Droughts of the Indian summer monsoon: role of clouds over the Indian Ocean. Curr Sci 85:1713–1719
Goswami BN (2005) Intraseasonal variability (ISV) of south Asian summer monsoon. In: Lau K, Waliser D (eds) Intraseasonal variability of the atmosphere–ocean climate system. Springer–Praxis, Chichester, pp 19–61
Goswami BN, Ajayamohan RS (2001) Intraseasonal oscillations and interannual variability of the Indian summer monsoon. J Clim 14:1180–1198
Hendon HH, Salby ML (1994) The life cycle of the Madden-Julian oscillation. J Atmos Sci 51:2225–2237
ICRP (2008) Continental Tropical Convergence Zone (CTCZ) Programme: Science Plan. DST, New Delhi
Jiang X, Waliser DE, Wheeler MC, Jones C, Lee M, Schubert SD (2008) Assessing the skill of an all-season statistical forecast model for the Madden–Julian oscillation. Mon Weather Rev 136:1940–1956
Jones C (2000) Occurrence of extreme precipitation events in California and relationships with the Madden-Julian oscillation. J Clim 13:3576–3587
Kalnay E et al (1996) The NCEP/NCAR 40-Year Reanalysis Project. Bull Am Meteorol Soc 77:437–471
Kistler R et al (2001) The NCEP–NCAR 50-Year reanalysis: monthly means CD-ROM and documentation. Bull Am Meteorol Soc 82:247–267
Knutson TR, Weickmann KM (1987) 30–60 day atmospheric oscillations: composite life cycles of convection and circulation anomalies. Mon Weather Rev 115:1407–1436
Knutson TR, Weickmann KM, Kutzbach JE (1986) Global-scale intraseasonal oscillations of outgoing longwave radiation and 250 mb zonal wind during northern hemisphere summer. Mon Weather Rev 114:605–623
Kripalani RH, Kulkarni A, Sabade SS, Revadekar J, Patwardhan SK, Kulkarni J (2004) Intraseasonal Oscillations during monsoon 2002 and 2003. Curr Sci 87:325–351
Krishnamurthy V, Shukla J (2000) Intraseasonal and interannual variability of rainfall over India. J Clim 13:4366–4377
Krishnamurthy V, Shukla J (2007) Intraseasonal and seasonally persisting patterns of Indian monsoon rainfall. J Clim 20:3–20
Krishnamurthy V, Shukla J (2008) Seasonal persistence and propagation of intraseasonal patterns over the Indian summer monsoon region. Clim Dyn 30:353–369
Krishnamurti TN, Ardunay P (1980) The 10–20 day westward propagating model and 'break' in the monsoon. Tellus 32:15–26
Krishnamurti TN, Bhalme HN (1976) Oscillations of monsoon system. Part I: observational aspects. J Atmos Sci 45:1937–1954
Krishnamurti TN, Subrahmanyam D (1982) The 30–50 day mode at 850 mb during MONEX. J Atmos Sci 39:2088–2095
Krishnamurti TN, Oosterhof DK, Mehta AV (1988) Air-sea interaction on the time scale of 30 to 50 days. J Atmos Sci 45:1304–1322
Lal M, Singh KK, Srinivasan G, Rathore LS, Naidu D, Tripathi CN (1999) Growth and yield responses of soybean in Madhya Pradesh, India to climate variability and change. Agric Forest Meteorol 93:53–70
Lau KM, Chan PH (1986) Aspects of the 40–50 day oscillation during the northern summer as inferred from outgoing longwave radiation. Mon Weather Rev 114:1354–1367
Liebmann B, Smith CA (1996) Description of a complete interpolated outgoing longwave radiation dataset. Bull Am Meteorol Soc 77:1275–1277
Love BS, Matthews AJ, Janacek GJ (2008) Real-time extraction of the Madden-Julian oscillation using empirical mode decomposition and statistical forecasting with a VARMA model. J Clim 21:5318–5335
Madden RA, Julian PR (1972) Description of global-scale circulation cells in the tropics with a 40–50-day period. J Atmos Sci 29:1109–1123
Madden RA, Julian PR (1994) Observations of the 40–50 day tropical oscillation: a review. Mon Weather Rev 112:814–837
Maharaj EA, Wheeler MC (2005) Forecasting an Index of the Madden-Julian oscillation. Int J Climatol 25:1611–1618
Mandke S, Sahai AK, Shinde MA, Susmitha Joseph, Chattopadhyay R (2007) Simulated changes in active/break spells during the Indian summer monsoon due to enhanced CO2 concentrations: assessment from selected coupled atmosphere–ocean global climate models. Int J Climatol 27:837–859
Meinke H, Stone RC (2005) Seasonal and inter-annual climate forecasting: the new tool for increasing preparedness to climate variability and change in agricultural planning and operations. Clim Change 70:221–253
Murakami M (1976) Analysis of summer monsoon fluctuations over India. J Meteorol Soc Jap 54:15–31
Pai DS, Rajeevan M (2009) Summer monsoon onset over Kerala: new definition and prediction. J Earth Syst Sci 118(2):1–13
Raghavan K (1973) Break monsoon over India. Mon Weather Rev 101(1):33–43
Raghavan K, Sikka DR, Gujar SV (1975) The influence of cross-equatorial flow over Kenya on the rainfall of western India. Q J R Meteorol Soc 101:1003–1004
Rajeevan M, Bhate J, Kale JD, Lal B (2006) High resolution daily gridded rainfall data for the Indian region: analysis of break and active monsoon spells. Curr Sci 91:296–306
Rajeevan M, Gadgil S, Bhate J (2008) Active and break spells of Indian Summer monsoon. NCC Research Report No. 7. India Meteorological Department, Pune, India
Ramage CS (1971) Monsoon meteorology, Academic Press, New York
Ramamurthy K (1969) Monsoon of India: some aspects of the 'break' in the Indian southwest monsoon during July and August. Forecasting Manual 1-57 No. IV 18.3. India Meteorological Department, Poona, India
RameshKumar MR, Krishnan R, Sankar S, Unnikrishnan AS, Pai DS (2009) Increasing trend of 'Break-Monsoon' conditions over India: role of ocean-atmosphere processes in the Indian Ocean. IEEE Geosci Remote Sens Lett 6(2):332–336
Rodwell MJ (1997) Breaks in the Asian Monsoon: the influence of Southern Hemisphere weather systems. J Atmos Sci 54:2597–2611
Shepard DA (1968) Two dimensional interpolation function for irregularly spaced data. In: Proc 1968 ACM Natl Conf, pp 517–524
Sikka DR, Gadgil S (1980) On the maximum cloud zone and the ITCZ over India longitude during the southwest monsoon. Mon Weather Rev 108:1840–1853
Singh SV, Kripalani RH (1985) The south to north progression of rainfall anomalies across India during the summer monsoon season. PAGEOPH 123:624–637
Singh SV, Kripalani RH (1986) Application of extended empirical orthogonal function analysis to interrelationships and sequential evolution of monsoon fields. Mon Weather Rev 114:1603–1610
Waliser DE, Weickmann K, Dole R, Schubert S, Alves O, Jones C, Newman M, Pan HL, Roubicek A, Saha S, Smith C, van den Dool H, Vitart F, Wheeler M, Whitaker J (2006) The experimental MJO prediction project. Bull Am Meteorol Soc 87:425–431
Webster PJ, Hoyos C (2004) Prediction of monsoon rainfall and river discharge on 15–30 day time scales. Bull Am Meteorol Soc 85:1745–1765

Webster PJ, Magana VO, Palmer TN, Shukla J, Tomas RA, Yanai M, Yasunari T (1998) Monsoons: processes, predictability, and the prospects for prediction. J Geophys Res 103:14451–14520
Wheeler MC, Hendon HH (2004) An all-season real-time multivariate MJO Index: development of an index for monitoring and prediction. Mon Weather Rev 132:1917–1932
Wheeler MC, McBride JL (2005) Australian-Indonesian monsoon. In: Lau WKM, Waliser DE (eds) Intraseasonal variability in the atmosphere-ocean climate system. Praxis Springer, Berlin, pp 125–173
Wheeler MC, Hendon HH, Cleland S, Meinke H, Donald A (2009) Impacts of the Madden-Julian oscillation on Australian rainfall and circulation. J Clim 22:1482–1498
Xavier PK, Goswami BN (2007) An Analog method for real-time forecasting of summer monsoon sub-seasonal variability. Mon Weather Rev 135:4149–4160
Yasunari T (1979) Cloudiness fluctuations associated with the northern hemisphere summer monsoon. J Meteorol Soc Jpn 57:227–242
Yasunari T (1980) A quasi-stationary appearance of 30 to 40 day period in the loudiness fluctuations during the summer monsoon over India. J Meteorol Soc Jpn 58:225–229
Yasunari T (1981) Structure of the Indian monsoon system with around 40-day period. J Meteorol Soc Jpn 59:225–229
Zhang C (2005) Madden-Julian oscillation. Rev Geophys 43:1–36